MODELS FOR PERMAFROST THICKNESS VARIATION IN RESPONSE TO CHANGES IN PALEOCLIMATE

J. P. GOSINK and T. E. OSTERKAMP

Geophysical Institute, University of Alaska in Fairbanks

Abstract

Three models were developed to determine the permafrost thickness response to changes in paleoclimate. Two models represent approximate numerical and analytical techniques to solve the heat balance equation at the permafrost base. The third model (finite element) numerically integrates the thermal energy equation from the surface, through the phase boundary, to the underlying thawed materials.

The amplitude of the permafrost thickness variation, A, depends directly on the amplitude of the surface temperature variation, ΔT, inversely on the geothermal heat flux, J, and inversely on the frequency of the surface temperature variation. For the thermal parameters and conditions used in the present study, the finite element model predicted a value of A which was reduced by as much as 30% from the approximate solutions in which J was assumed constant (from 78m to 51 m).

The lag, ß, between surface temperature and permafrost thickness response increases with frequency, soil porosity, and ΔT, and decreases with increasing J. All three models predict a lag of about 19 130 years. The permafrost response includes an initial transient which has a time-scale, t_a of about 41 186 years which increases with soil porosity and ΔT, and decreases with increasing J.

In response to sinusoidal surface temperature, the phase boundary is displaced asymmetrically with faster thawing than freezing. This also produces asymmetry in the maximum and minimum permafrost thicknesses.

Résumé

Trois modèles ont été mis au point pour déterminer le résultat des changements paléoclimatiques sur l'épaisseur du pergélisol. Deux modèles font appel à des techniques analytiques et numériques approximatives pour résoudre l'équation du bilan thermique à la base du pergélisol. Le troisième modèle (éléments finis) intègre numériquement le transfert de l'énergie thermique à partir de la surface et son passage à travers les limites de changement de phase jusqu'aux matériaux dégelés sous-jacents.

L'amplitude de la variation d'épaisseur du pergélisol, A, dépend directement de l'amplitude de la variation thermique à la surface, ΔT, inversement au flux géothermique, J, et inversement de la fréquence des variations thermiques à la surface. Avec les paramètres et les conditions thermiques employés dans la présente étude, le modèle des éléments finis prédit une valeur de A jusqu'à 30 % plus faible à partir des solutions approximatives dans lesquelles J était supposé constant (de 78 m à 51 m).

Le décalage, ß, entre les températures de surface et les variations de l'épaisseur du pergélisol augmente avec la fréquence, la porosité du sol et ΔT, et diminue à mesure que J augmente. Les modèles prédisent tous trois un décalage d'environ 19 130 années. La réaction du pergélisol comprend un état transitoire initial possédant une échelle de temps t_a d'environ 41 186 années qui augmente avec la porosité du sol et ΔT, mais qui diminue à mesure que J augmente.

En réponse à l'oscillation sinusoïdale de la température de surface, la limite de phase est déplacée asymétriquement en fonction d'un dégel plus rapide que l'engel. Cela produit aussi une certaine asymétrie dans les épaisseurs maximale et minimale du pergélisol.

Introduction

Permafrost is a product of cold climates that cause it to grow from the ground surface downward. The first permafrost on earth must have formed prior to or coincident with the first glaciation which, according to Frakes (1979), occurred about 2.3 billion years ago. Permafrost occurrences and distribution may be expected to increase during periods of glaciation and to decrease during warm intervals. In Alaska, there is no reported evidence for the occurrence of permafrost in continental lowland areas prior to 2.5 million years ago. Carter *et al.* (1986) suggest that current permafrost in Alaska was initiated during the climatic deterioration that began about 2.5 million years ago and which led into the first (recent) major glaciation of the Northern Hemisphere. During the past million years there is evidence for repeated glaciations with a periodicity of about 105 years (Shackleton and Opdyke, 1977).

There are two time scales of concern for the response of permafrost to changes in climate (i.e., to changes in temperature at the permafrost table). The first time scale is the time required for the temperature profile in the permafrost to adjust to a new surface temperature. This time scale, t_c is on the order of (Lachenbruch *et al.*, 1982; Osterkamp, 1983)

$$t_c \approx \frac{X^2}{4D} \qquad (1)$$

where X is the thickness of the permafrost and D is its thermal diffusivity. For most permafrost, t_c ranges from a few years to about 3×10^3 yr. However, when there is a significant amount of unfrozen soil solution in the permafrost, t_c may become much larger because of latent heat associated with the change of phase when the temperature of the permafrost changes. The second time scale is the time required for the permafrost thickness to respond to changes in surface temperature. After the initial transient response of the temperature profile (on the order of t_c) the permafrost may be expected to thaw at a rate on the order of 1 cm per year because of geothermal heat flow into the base. Consequently, for a sudden change in surface temperature of thick continuous permafrost, several tens of thousands of years may be required for the permafrost thickness to adjust to the new surface boundary condition. Such long times are a significant fraction of the periodicity of recent glaciations. It is, therefore, of interest to begin to examine the thickness response of permafrost to changes in paleoclimate to determine the current state of the permafrost thickness (i.e., whether the permafrost is currently freezing, thawing or near equilibrium). This paper presents some preliminary results from analytical and numerical models developed for this purpose.

Approximate solutions

The position of the phase boundary between frozen and thawed soils, X(t), can be determined from two boundary conditions (Carslaw and Jaeger, 1959):

$$T_1 = T_2 = T_f, \text{ when } x = X(t) \qquad (2)$$

and

$$K_1 \frac{\partial T_1}{\partial x}\bigg|_{x=X(t)} - K_2 \frac{\partial T_2}{\partial x}\bigg|_{x=X(t)} = L\rho_i\theta \frac{dX}{dt} \qquad (3)$$

where t is time, x is depth measured downward and the region $x<X(t)$ represents frozen soil with temperatures $T_1(x,t)$ and thermal conductivity K_1, and the region $x>X(t)$ represents thawed soils with temperatures $T_2(x,t)$ and thermal conductivity K_2. The latent heat, L, is associated with the change of phase of soil moisture, θ is the soil water content, ρ_i is the density of the unfrozen water, and T_f is the phase equilibrium temperature or the freezing-point-depression. Equation (2) specifies continuity of the temperature at the phase-boundary, and (3), which is non-linear, represents a balance between heat conducted to or from phase boundary, and heat generated or absorbed there by change of phase.

A difficulty in determining the position of the phase boundary from (2) and (3) arises from the variability of the temperature gradients in both the frozen and the thawed zones. However, if these temperature gradients vary in a predictable manner, it is possible to solve (3) for X(t). Estimates for $\partial T_1/\partial x$ and $\partial T_2/\partial x$ are developed below to obtain approximate solutions of (3).

Thermal gradient in the ice-bearing permafrost.

When a temperature change is introduced at the surface of the permafrost, the thermal response of the frozen soil occurs within about t_c. For a layer with fixed thickness X and constant temperature at the base, the permafrost temperatures will be within 84 % of their final state when $t \approx t_c$ (Carslaw and Jaeger, 1959). A layer of permafrost which is 600m deep with a thermal diffusivity of $50 m^2 yr^{-1}$ will adjust to a surface disturbance within about 1800 years. Time scales of importance for paleoclimatic studies of permafrost range from millennia to 2 or 3 million years. In particular, for this study, a cyclic temperature disturbance is assumed at the permafrost surface with a period of 100 000 years. Then, since t_c is only a small fraction of this period, as a first approximation it is reasonable to assume that temperatures in the permafrost respond immediately to the sinusoidal forcing at the surface, and consequently that the temperature gradient in the layer is linear with depth. A similar approach has been developed by Osterkamp *et al.* (1987) for the interpretation of data on subsea permafrost. This approach provides an estimate for the temperature gradient in the permafrost, $\partial T_1/\partial x \approx [T_f - T_s(t)]/X(t)$ where the surface temperature, $T_s(t) = T_m + \Delta T \sin \omega t$, T_m is the mean surface temperature, and ΔT is the amplitude of the surface temperature variation.

Thermal gradient below ice-bearing permafrost.

The temperature gradient in the thawed soil below the ice-bearing permafrost is due to the geothermal heat flux. This flux has generally been assumed to be constant in earlier models for prediction of the permafrost thermal regime (Lachenbruch, 1988) and will also be assumed constant herein. This approximation will be examined more closely in comparisons with a complete numerical solution. The above estimates for temperature gradients in the frozen and thawed layers lead to:

$$L\rho_i\theta \frac{dX}{dt} = K_1\left[T_f - T_m - \Delta T \sin \omega t\right] / X - J \qquad (4)$$

where J is the assumed constant geothermal heat flux. Equation (4) is a first order non-linear ordinary differential equation which can be solved for X(t) by numerical integration or by a perturbation technique. The solution of (4) requires one initial condition, $X(t=O)=X_i$

SOLUTION BY A FINITE DIFFERENCE METHOD.

A straightforward explicit finite difference method was used to integrate (4). We have tested the method with a range of time steps, and found little or no difference between solutions when the time step was less than about 500 years. The solution for X(t) using this method with a time step of

500 years is depicted by the solid curve in Figure 1. For this example, it was assumed that the initial permafrost depth X_i=600m, T_f=-1 °C, T_m=-11 °C, ΔT=4 °C, K_1=3.39 $Wm^{-1}°C^{-1}$, θ=0.4, $\rho_i L$=3.06 x 10^8 Jm^{-3}, and J=0.0565 Wm^{-2}. Predicted permafrost depths are characterized by an initial transient thinning which damps out within one or two cycles of the surface oscillation. The subsequent predicted permafrost thickness appears to follow a relatively steady periodic asymmetric pattern, such that 510m≤X≤684m. The surface reaches its maximum temperature 25 000 years from the start of a cycle, and from Figure 1 it appears that the permafrost reaches its minimum thickness after about 45 000 years, implying a lag between surface forcing and the response of the permafrost thickness of about 20 000 years. With periodic forcing, the predicted change in permafrost thickness is 90m for this approximate solution as compared with the expected long-term change of 240m when the surface temperature is impulsively altered by ± 4 °C.

Solution by a perturbation method.

Perturbation techniques provide X = X(t), which yields systematic information on the expected amplitude, phase, lag and attenuation of X(t) in terms of the imposed surface temperature variation. A perturbation solution for X(t) was determined by assuming an expansion in terms of a small parameter λ such that:

$$X(t) = X_0+\lambda X_1(t)+\lambda^2 X_2(t)+\lambda^3 X_3(t)+\ldots \qquad (5)$$

This expression is substituted into (4), and a series of equations in like powers of λ is generated (for example, see Nayfeh, 1973). The zeroth order solution is $X_O = K_1(T_f-T_m)/J$, a constant. This is the long-term periodic mean thickness and is also the steady state solution when ΔT=O. Note that the zeroth order solution does not in general satisfy the initial condition. The first order solution is:

$$X = X_o + \lambda X_1(t)$$

$$=K_1(T_f-T_m)/J$$

$$-A \sin(\omega t-\beta) + [X_i-K_1(T_f-T_m)/J)-A \sin\beta]\exp(-t/t_a) \qquad (6)$$

where $t_a = L\rho_i\theta X_o/J$ is a transient time-scale, the lag angle $\beta = \arctan(\omega t_a)$, and the amplitude of the displacement of the permafrost thickness:

$$A = K_1\Delta T / J\sqrt{1+(\omega t_a)^2} \qquad (7)$$

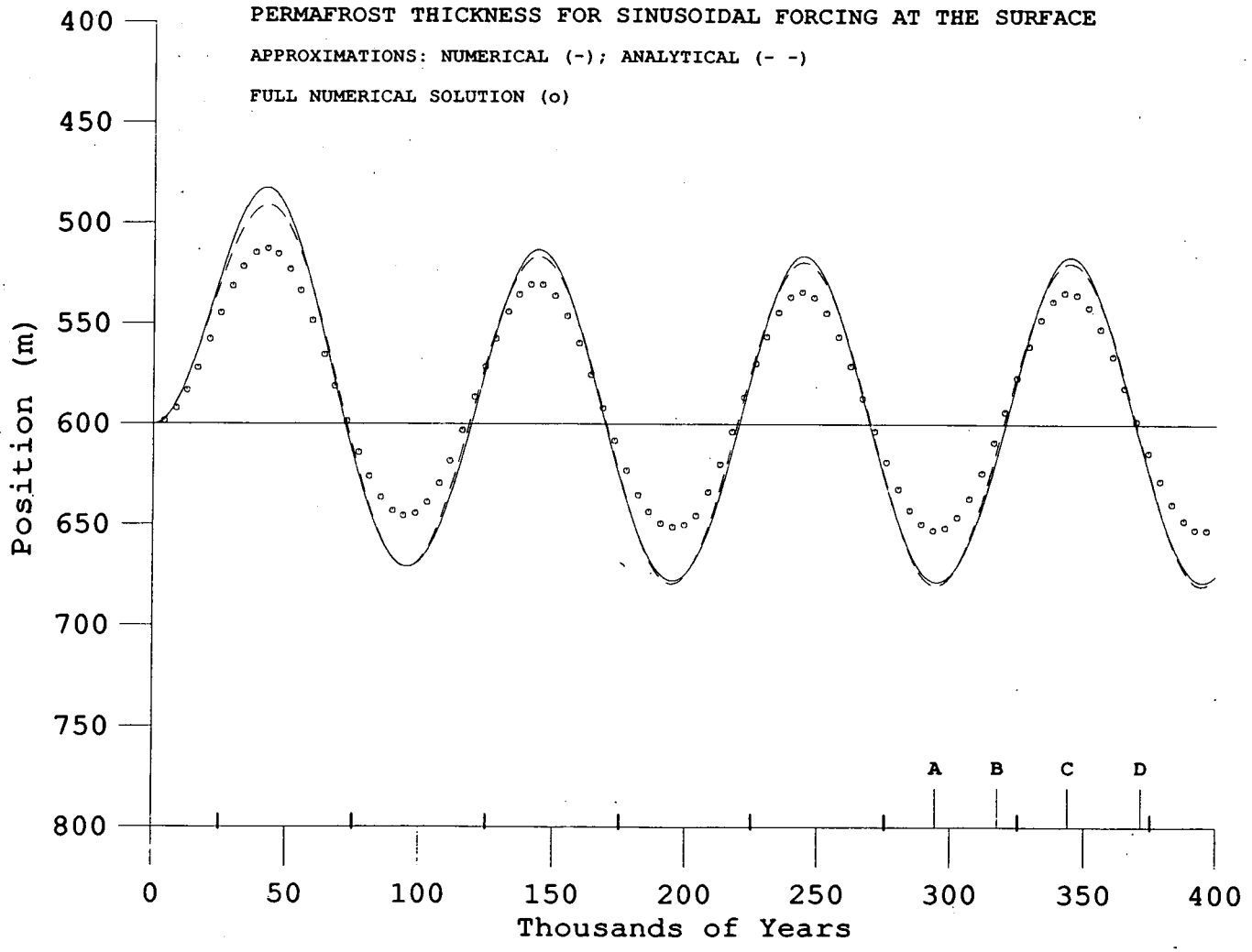

Figure 1. Permafrost thickness versus time for sinusoidal temperatures at the permafrost surface. Approximate numerical method (—); perturbation solution (--); finite element method (o).

This solution satisfies the initial condition, $X(t = 0) = X_i$. Equation (6) (dashed curve in Figure 1) displays the amplitude, phase, lag and attenuation of the function X(t) explicitly. This first order perturbation solution appears to be a very good estimate of the numerical solution for (4). The magnitude of the largest term in the second order perturbation solution is about 3m for the above thermal constants and parameters. Therefore, taking only the first order term in the linearized perturbation expansion produces reasonably good agreement with the numerical solution.

From (7), A is directly proportional to ΔT, and inversely proportional to J. High frequency changes in surface temperature (short period events) result in smaller variations of the permafrost thickness than low frequency changes of the same magnitude. Using the values of the thermal constants listed above, A≈86.5m. The sinusoidal response of X(t) in (6) also provides an estimate of dX/dt; the maximum value of dX/dt after the initial transient is $\omega \cdot A \approx 5\text{mm yr}^{-1}$.

The lag, ß, depends inversely on the squared magnitude of J and directly upon the product of the soil porosity and latent heat. However, the perturbation method is not applicable in the limiting case of J = 0, which is the standard Stefan solution. For the thermal constants and parameters used in the present example, ß≈ 68.9°, implying a lag of about 19 130 years, very close to the estimate obtained from the graph of the numerical solution.

The transient time scale, t_a represents the time required for the permafrost thickness to adjust to the sinusoidal surface temperature variation and establish a regular periodic behavior. In this case, t_a≈41 186 years, suggesting that the permafrost thickness adjusts to the initial disturbance within one cycle, subsequently following a simple sinusoidal displacement but lagging the surface temperature by ß. As expected, t_a increases with increasing soil porosity, and decreases with J. Both t_a and ß increase as $T_f - T_m$ increases. Thus, colder regions require a longer period of adjustment to any variation in the surface temperature. This initial adjustment can be clearly seen in Figure 1, where during the first cycle, the permafrost thickness predicted by the perturbation method decreases to about 490m. The difference between this thickness and the predicted minimum long-term permafrost thickness (513.5m) is determined from the two terms which comprise the coefficient of the exponential term in (6). The first of these, $X_i - X_O$, is the deviation of the prescribed initial thickness from the long-term periodic mean thickness. The second, A sin ß, decreases as the frequency of the thermal forcing at the surface increases, implying that this initial transient is smaller for very long-period surface forcing.

Finally, for completeness, the second order solution, $\lambda^2 X_2(t)$, is:

$$\lambda^2 X_2(t) = \frac{-A^2 \sin\gamma}{4X_o}\sin[2\omega t - 2\beta - \gamma] - \frac{[\Delta X - A\sin\beta]^2}{X_o}\exp(-2t/t_a)$$
$$+\frac{A\csc\beta}{X_o}[\Delta X - A\sin\beta]\cos(\omega t - \beta)\exp(-t/t_a) \qquad (8)$$
$$+\left\{\frac{-A^2\sin\gamma\sin(2\beta+\gamma)}{4X_o} + \frac{[\Delta X - A\sin\beta]}{X_o}[\Delta X - A\cos\beta\cot\beta]\right\}\exp(-t/t_a)$$

where $\tan\gamma = 2\tan\beta$ and $\Delta X = X_i - X_O$. From this expression, the magnitude of the non-decaying periodic term, $A^2/4X_o \approx 2.7$m. Note that for these parameters, $\gamma \approx 80°$, meaning that the leading term in the second order solution behaves similar to a $\cos[2\omega)t - 2\beta]$ function. This implies that the leading term in the second order solution decreases both the minimum and the maximum thicknesses predicted by the first order solution, or in other words, the leading term adjusts the perturbation solution such that it tends to converge to the numerical solution.

The numerical solution depicted in Figure 1 is not perfectly symmetric: thickening excursions are slower than thinning excursions. That is, for each half-cycle of the period, dX/dt is smaller when X is large than when X is small. Figure 2a shows the magnitude of dX/dt (small circles) concurrently with X as computed with the numerical method for two cycles after the initial transient. A mean sinusoidal curve (solid curve) has been drawn through the calculated values of |dX/dt| for reference. The figure shows the faster velocities of the phase boundary associated with thinning events (X<600m) and the slower velocities associated with thickening events (X>600m). This feature is implicit in (4) where it can be seen that the magnitude of dX/dt is inversely proportional to X. In contrast, the first order perturbation solution given by (6) follows a symmetric sinusoidal function after the initial transient time scale. Thus, the first order perturbation solution shown as the dashed curve in Figure 1 is symmetric, and deviates from the numerical solution in such a way as to be narrower during thickening and slightly wider during thinning. Since the leading term in the second order perturbation solution approximates a $\cos[2\omega)t - 2\beta]$ function, this term tends to correct the symmetry of the total perturbation solution by adding slower thickening excursions and faster thinning excursions.

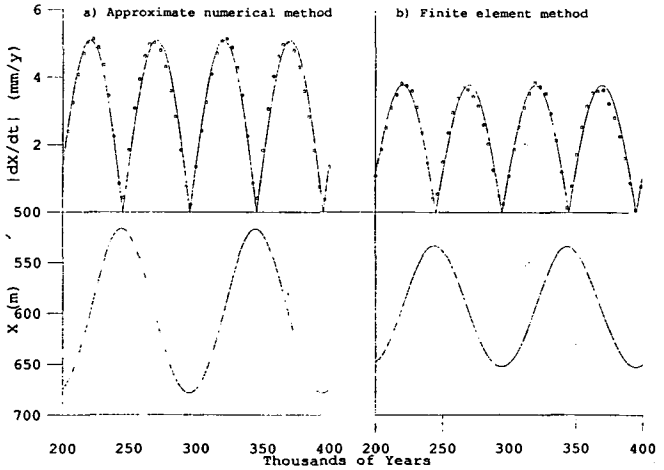

Figure 2a. |dx/dt| and X versus time calculated with the approximate numerical method. Top graph: |dx/dt| (o); mean sine curve (—). Bottom graph: X (o o o).

Figure 2b. |dx/dt| and X versus time calculated with the finite element method. Top graph: |dx/dt|(o); mean sine curve (—). Bottom graph: X (o o o).

Finally, note that this asymmetry in the rates of thickening and thinning (i.e., in dX/dt) also results in the asymmetry of the maximum and minimum thicknesses. The long-term mean thickness for this example is 600m. Therefore, the area in Figure 1 between the thickening curve and the X = 600m line should equal the area between the thinning curve and the X = 600m line. Thus, since the thickening curves are wider than the thinning curves, the maximum displacement from 600m during thickening must be less than that during thinning. This agrees with the predicted maximum thickness of 684m (displacement is 84m) and the predicted minimum thickness of 510m (displacement is 90m). Study of these asymmetries is continuing.

The perturbation solution is a close approximation to the numerical solution and appears to converge to it. However, it should be noted that the assumption of a linear temperature profile in the permafrost and a constant value for J provides only an approximation of the permafrost thickness response. In order to determine the response more precisely, it is necessary to solve the complete heat flow equation with appropriate boundary conditions, and this requires a numerical model. The development of a complete finite element model for heat flow in permafrost and the predictions of that model are presented in the following section.

Full numerical solution

A complete numerical solution to the heat flow equation provides an "exact" method for determining the position of the phase boundary for arbitrary surface conditions. However, the exactness of the solution depends upon both the correctness of the assumptions implicit in the model and the details of the numerical method. This section presents the results of the application of a finite element model to the problem of sinusoidal surface boundary conditions. The model has been extensively tested against analytic solutions over long time scales (Gosink, unpublished research). Application of the model to the problem of long-term response of the permafrost to changes in paleoclimate requires specification of the appropriate boundary conditions and thermal parameters for the permafrost and the underlying thawed soil. If lateral changes in the temperature of the ground surface can be ignored, then:

$$\frac{\partial H}{\partial t} = K\frac{\partial^2 T}{\partial x^2} \qquad (9)$$

where the enthalpy change ΔH associated with a change in temperature is:

$$\Delta H = \int \rho C_p dT + \int d\theta(T) L(T) \qquad (10)$$

T is temperature, ρ is bulk density, C_p is the composite soil specific heat, K is the composite thermal conductivity of the soil, and $\theta(T)$ is the volume fraction of unfrozen water or brine which may be a function of temperature, and L(T) is the volumetric latent heat, which is described in more detail below.

The finite element model used in these calculations was specifically devised for paleoclimatic studies; it includes options for temperature- and salinity-dependent soil thermal properties, adjustable weighting of the spatial differences permitting implicit, Crank-Nicolson or other differencing methods, and double-precision calculations. The last refinement was found to be necessary for calculations taken over the long time-scales involved in these investigations of paleoclimate effects on the permafrost. Latent heat is included by either of two methods, that of Osterkamp (1987) which uses an effective specific heat containing latent heat as a source distributed over a given temperature range, and a method developed by O'Neill (1983 a and b) which employs a latent heat content 'spike' at a given freezing temperature. In the present study, for comparison of these calculations with the approximate solutions, we have used constant values of the soil thermal parameters in both the thawed and frozen regions and the latent heat content spike approach. Values of the thermal parameters are determined during the course of the calculations, depending upon the position of the phase boundary.

Using the finite element model, predictions were obtained for the thickness response of the permafrost to an imposed sinusoidal temperature at the permafrost surface; these are depicted by the small circles in Figure 1. The displacements predicted with the finite element model are similar to the displacements obtained by the approximate methods of the previous section in terms of phase and lag, but the magnitudes of these displacements are considerably reduced. An explanation for this reduction in magnitude can be found by considering the effect of heat flux, and in particular, the local temperature gradients, at the position of the phase boundary.

Temperature profiles calculated with the finite element method at four times, 294 500, 317 500, 344 000 and 371 500 years are displayed in Figure 3. These times correspond approximately to the occurrence of maximum, mean, minimum and mean permafrost thickness, in the sequence of thinning followed by thickening (see Figure 1). The permafrost thickness for a full cycle varies between $531m \leq X \leq 657m$.

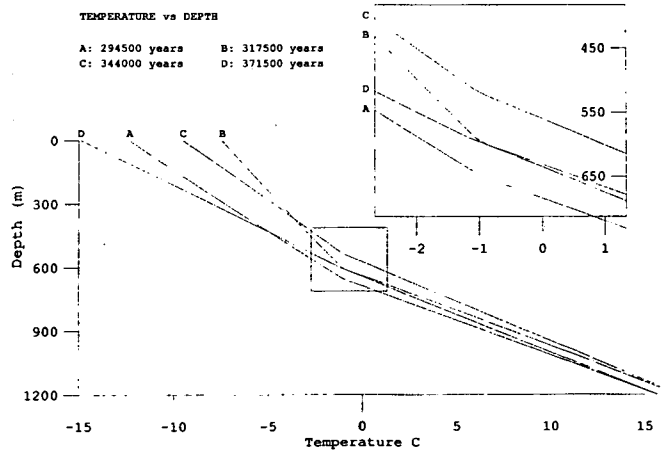

Figure 3. Temperature versus depth at 294 500, 317 500, 344 000 and 371 500 years calculated with the finite element method.

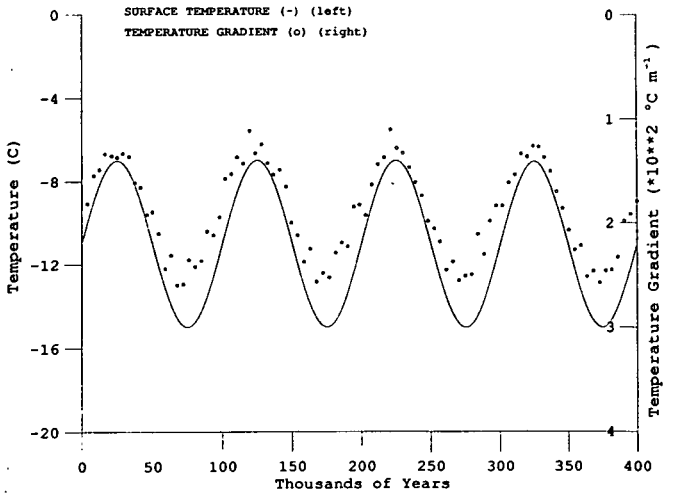

Figure 4. Surface temperature (—) and $\partial T_1/\partial x(o)$ as calculated by the finite element method.

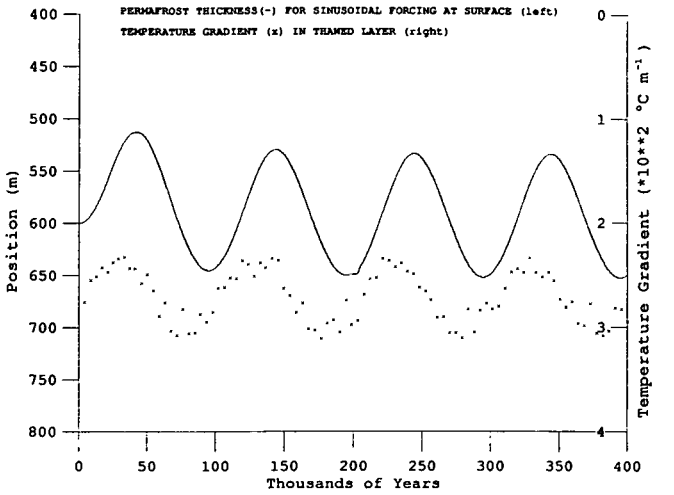

Figure 5. X (—) and $\partial T_2/\partial x(x)$ as calculated by the finite element method.

Figure 3 shows the near-linearity of the temperature profiles in permafrost, supporting that assumption for the approximate methods. Other evidence supporting the assumption of linear gradients in the permafrost is presented in Figure 4 where the in-phase relation between the temperature gradient near the phase boundary (as calculated by the finite element method) and the temperature at the ground surface is displayed. The rapid adjustment of temperatures in the permafrost to surface forcing is due to the relatively small value of $t_c \approx 1800$ yr. These gradients show some scatter since they were obtained from a fairly coarse grid (10m) as the calculated temperature difference divided by the position difference between the phase boundary and the nodal point depth. The magnitude of the gradient can show anomalous behavior as the phase boundary position approaches a nodal point. To minimize these anomalies, nodal points one position away from the phase boundary were used for differencing in Figure 4. However, even with the remaining scatter, the periodicity, which is in-phase with the surface temperature, as well as the typical range of variation of the temperature gradient, are apparent in the figure.

When the permafrost thickness decreases, we anticipate that the temperature gradient in the thawed material will decrease in magnitude near the phase boundary as the temperature profile curves upward from a constant gradient at great depth to the relatively shallow position of the phase boundary. Conversely, when the permafrost thickness increases, the temperature profile curves downward in the thawed layer from the constant gradient at depth to the relatively deeper position of the phase boundary. The net effect is a decrease of the bottom temperature gradient and associated heat flux to the phase boundary during thawing, and an increase of the bottom temperature gradient and heat flux during freezing. During thawing, less heat is conducted to the phase boundary from below (relative to a long-term mean at depth), and during freezing, more heat is conducted to the phase boundary from below. Physically this means that part of J goes into warming the permafrost below the phase boundary during warming and more heat is removed through permafrost from below the phase boundary during cooling. This implies that the displacement of the phase boundary is modified by the local variations in bottom temperature gradient in such a way as to attenuate that displacement. Effectively, it is the periodic variation in this heat flux which attenuates the displacement of the phase boundary. The phase relationship between permafrost thickness and the magnitude of the temperature gradient in the thawed layer can be tested by examining these parameters as calculated by the finite element method; numerical predictions of X and temperature gradient in the thawed layer are shown in Figure 5. The figure demonstrates that the gradient reaches a maximum value some time before the permafrost reaches maximum thickness and it reaches a minimum value some time before the permafrost reaches minimum thickness. This implies that maximum heat is conducted to the phase boundary slightly before the permafrost reaches maximum thickness, and minimum heat is conducted there slightly before the permafrost reaches minimum thickness. However, even with this deviation in timing from the in-phase relation, it is clear from Figure 5 that the heat flux is somewhat higher than a long-term mean value when the permafrost reaches maximum thickness and this results in less thickening, and that the heat flux is somewhat lower than the longterm mean value when the permafrost reaches minimum thickness resulting in less thinning. In this way, the local periodicity of the geothermal heat flow serves to attenuate the displacement of the phase boundary.

The exact solution shown in Figure 1 reveals that this solution, like the approximate solution, is asymmetric, with slightly slower thickening excursions and slightly faster thinning excursions. This can also be seen in Figure 2b where $|dX/dt|$ and X as calculated by the finite element method are displayed. A mean sinusoidal curve has been drawn through the calculated values of $|dX/dt|$ showing the larger velocities when X <600m, and smaller velocities when X >600m. The reason for this behavior is the same as for the approximate solution: the magnitude of $\partial T_1/\partial x$ is smaller when X is large (heat must be removed from more

soil by conduction) and consequently, the magnitude of dX/dt is smaller when X is large. A secondary consequence, as explained previously, is the asymmetry in the maximum values of the displacement during thickening and thinning. Thus, according to the finite element model, the maximum predicted thickness is 657m (displacement is 56m), and the minimum predicted thickness is 531m (displacement is 69m). However, it should be noted that the magnitude of the asymmetry is larger for the finite element solution (69-57 = 12m) than for the approximate numerical solution (90-84 = 6m). This suggests that the periodic variation in the heat flow from the thawed soil also affects the phase boundary velocities in such a way as to reduce thickening relative to thinning. Study of this feature is continuing.

Conclusions

Three models were developed to determine the variation in permafrost thickness in response to changes in paleoclimate. The first two models represent two approximate methods, involving numerical and analytical techniques, to solve the heat balance equation at the phase boundary by assuming constant geothermal heat flux and linear temperature profiles in the permafrost. The third model is a complete numerical scheme using finite elements to numerically integrate the thermal energy equation from the surface, through the phase boundary, to the underlying thawed materials. Comparison of the three solutions provides complementary information on the response of the permafrost thickness to variations in surface temperature.

The analytic method has the advantage of providing an explicit function, X(t), with general expressions for the amplitude, phase, lag and initial transient response of the permafrost to sinusoidal surface temperature. Thus, through the analytic method, it can be shown that the amplitude of the permafrost thickness displacement, A, depends directly on the magnitude of the surface temperature variation, ΔT, inversely on the geothermal heat flux, J, and inversely on the frequency of the surface temperature variations. With both approximate methods, the heat flux from the thawed material is assumed to be constant, and with the finite element method, the variations in the heat flux are calculated by the model. Since heat flux from the thawed material reaches a maximum value as the permafrost is thickening and a minimum value as the permafrost is thinning, the finite element model predicts that the variation in permafrost thickness is attenuated. For the thermal parameters and conditions used in the present study, this was a significant attenuation, reducing the displacement of the permafrost by about one third from the approximate solution (from 84m to 57m). Furthermore, the magnitude and phase of the temperature gradients in the permafrost near the phase boundary as calculated with the finite element method agree substantially with the gradients assumed in both of the approximate methods.

The lag, β, between surface temperature and permafrost thickness response increases with frequency of the surface temperature variations, soil porosity, and ΔT, and decreases with increasing J. For the thermal parameters and boundary conditions used in this study, the analytic solution predicts a lag of 19 130 years, and this value was verified by the approximate numerical and finite element models. The permafrost response includes an initial transient which has a time-scale, t_a of about 41 186 years. According to the analytic solution, ta increases with soil porosity and ΔT, and decreases with increasing J.

Finally, the phase boundary is displaced asymmetrically in response to sinusoidal surface temperature, with faster thinning excursions than thickening excursions. Since the long-term mean permafrost thickness is constant, this also produces asymmetry in the maximum and minimum permafrost thicknesses. The asymmetry is apparent in both the approximate methods and in the complete finite element method. However, the asymmetry in thickness is larger with the finite element method than with the approximate methods, suggesting that the variation in heat flow from the thawed soil also affects the phase boundary velocities in such a way as to reduce thickening relative to thinning.

Acknowledgements

We wish to thank T. Fei and T. Zhang for their help with the numerical calculations. This research was sponsored by the Earth Sciences Section, Division of Polar Programs, National Science Foundation under Grants No. DPP86-19382 and DPP87-21966 and U.S. Geological Survey Award No. 14-08-001-G1305

References

CARSLAW, H. S., AND J. C. JAEGER, 1959. Conduction of heat in solids, Oxford University Press, London.

CARTER, L. D., J. BRIGHAM-GRETTE, L. MARINCOVICH, V. L. PEACE, AND J. W. HILLHOUSE, 1986. Late Cenozoic Arctic Ocean sea ice and terrestrial paleoclimate, Geology, 14 675-678.

FRAKES, L. A., 1979. Climates throughout geologic time, 310 pp. Elsevier, New York.

LACHENBRUCH, A. H., J. H. SASS, B. V. MARSHALL, AND T. H. MOSES, JR., 1982. Permafrost, heat flow, and the geothermal regime at Prudhoe Bay, Alaska, J. Geophys. Res., 87(B11), 9301-9316.

LACHENBRUCH, A. H., T. T. CLADOUHOS, AND R. W. SALTOS, 1988. Proceedings of the Fifth International Conference on Permafrost, Tr^0ndheim, Norway.

NAYFEH, A. H., 1973. Perturbation methods, John Wiley and Sons, N.Y.

O'NEILL, K., 1983a. Solutions of 2-D axisymmetric phase change problems on a fixed mesh, with zero phase change width, Proceedings of the Third International Conference on Numerical Methods in Thermal Problems, Seattle, WA.

O'NEILL, K., 1983b., Fixed mesh finite element solution for Cartesian 2-D phase change, J. Energy Res. Tech., 105, 436-441.

OSTERKAMP, T. E., 1983. Response of Alaskan permafrost to climate, Proceedings of the Fourth International Conference on Permafrost, Final proceedings, National Academy Press, Washington, D.C., 145-151.

OSTERKAMP, T. E., W. D. HARRISON, AND D. M. HOPKINS, 1987. Subsea permafrost in Norton Sound, Alaska, Cold Regions Science and Technology, 14,173-180.

OSTERKAMP, T. E., 1987. Freezing and thawing of soils and permafrost containing unfrozen water or brine, Water Resour. Res., 23(12), 2279-2285.

SHACKLETON, N. J., and N. D. OPDYKE, 1977. Oxygen isotope and paleomagnetic evidence for early northern hemisphere glaciation, Nature, 270, 216-219.